AN APPROACH TO HUMAN ARM MOTION TRACKING USING INERTIAL SENSORS

Ningxia Yang*, Min Qin and Yan Wang

Department of Computer Application Engineering
Hebei Software Institute
No. 1, Zhida Road, Baoding 071000, P. R. China
*Corresponding author: luozhangyulong@163.com

ABSTRACT. *This paper presents an approach to track the human body arm movements using inertial sensors. Human arm is modeled as a multi-link kinematic chain which consists of shoulder joint, elbow joint and wrist joint, connected by upper arm and forearm respectively. The Lie algebra techniques: twists and exponential maps that are able to map the joint quaternions to joint positions are adopted to track the arm movements. The real-time inertial data transmission to the host computer is through Bluetooth technique. The optical tracking device OptiTrack, which features in sub-millimeter accuracy, is utilized in evaluating the accuracy of our inertial tracking system. The experimental results demonstrate the feasibility and viability of our proposed arm motion tracking approach.*
Keywords: Arm motion tracking, Lie algebra, Twists and exponential maps, Inertial sensor, Bluetooth communication

1. **Introduction.** As the proliferation of the MEMS (micro-electro-mechanical system) technology enables the compact and wearable sensors, the inertial based motion tracking methods are being conducted in a variety of research areas such as virtual reality, athlete daily training, post-stroke patient rehabilitation, lost motor function recovery and elderly daily exercise monitoring [1, 2, 3, 4, 5].

Inertial sensor that consists of accelerometers, gyroscopes and magnetometers characterizes in long-term mobility, quick response and non-invasiveness in the free living environments [5, 6]. However, the inertial sensor inherently suffers from long-term drifting problem especially being worn on the human body for daily rehabilitation [7]. Due to that reason, MEMS based motion tracking is still unsuitable for pervasiveness among the general public rehabilitation in the free living environments.

A human body includes torso, head, upper arms, forearms, hands, thighs, shanks and feet [9]. Compared with the other body segments, the limb segments perform more complicated movements that exert challenging tasks in achieving long-term MEMS based motion tracking [3, 10]. Human upper limbs and lower limbs have similar structures but distinct functionalities. The movements performed by upper limbs prove to be more sophisticated and dimensional than those of lower limbs. For the reasons given above, we choose to capture the arm motions using inertial sensors and to evaluate the system accuracy using sub-millimeter accurate visual tracking system: *OptiTrack* [11].

Quite a few researches have been focused on the motion tracking areas recently [8, 13]. The estimation of joint angles from inertial sensors using Denavit-Hartenberg representation is introduced in [12]. In [10], the human arm kinematic model is adopted and inertial based forearm position and orientation are estimated. The positions of arm joints are calculated individually without taking the multi-link constraints into account which,

to some extent, lowers the estimation accuracy. Generally, the state-of-the-art inertial-based motion tracking methods are still low in accuracy and suffer from long-term drifting problems. There still exist some potential areas for the further exploration.

In this paper, we propose the Lie-algebra based arm motion tracking approach using inertial sensors, specifically, the mathematical formulations: twists and exponential maps are exploited to describe the arm motions. Experimental results show that our proposed arm motion tracking method perfectly recovers the movement process. The highly accurate vision tracking device *OptiTrack* is utilized and applied to verifying the deduced joint position accuracy using coordinate transformation technique.

The rest of the paper is summarized as follows. In Section 2, the arm motion tracking method is presented, followed by coordinate transformation in Section 3. Experimental results and analysis are introduced in Section 4. Ultimately, conclusions are presented in Section 5.

2. **Arm Motion Tracking.** Researcher Charles pointed out that a rigid body can be moved from any one place to any other by a movement, which consists of rotation and transition [14]. Rigid motion has the elegant property that preserves the distance between two points and the angle between the vectors.

2.1. **Kinematic modeling.** Human upper limbs can be modeled as a kinematic chain which consists of three rigid body segments, three joints and seven degrees of freedom (DoFs). Shoulder is described as a ball with three DoFs; elbow is modeled as two hinge joints with tow DoFs; wrist is modeled as an ellipsoid with two DoFs. In our inertial arm motion tracking system, inertial sensors are mounted adjacent to the right arm joints, i.e., wrist, elbow and shoulder [10]. During the inertial sensor configuration, the consideration on lowering the effects of soft tissue artifacts should be taken.

2.2. **Inertial sensor configuration.** In our tracking system, three coordinate frames are taken into account. These are shoulder joint coordinate frame, elbow joint coordinate frame and wrist joint coordinate frame. The shoulder joint is assigned to be the base frame linking a succession of upper arm and forearm movements. The instantaneous position and orientation of the wrist and elbow joint, relative to the shoulder inertial frame, can be represented by the pair $\{P_{ab}, R_{ab}\}$, where P_{ab} is the vector from the origin of shoulder coordinate frame to wrist/elbow frame. R_{ab} is the rotation of wrist/elbow frame relative to the shoulder frame.

2.3. **Twists and exponential maps.** As we have mentioned in the above, the pair $\{P_{ab}, R_{ab}\}$ describes the relationship (translation and rotation) of the inertial frame B relative to inertial frame A. More precisely, Let q_a and q_b be the coordinates of point Q in the frame A and B respectively. Then q_a and q_b satisfy the following equation.

$$q_b = P_{ab} + R_{ab}q_a \tag{1}$$

The homogeneous representation of the above equation is

$$\begin{bmatrix} q_a \\ 1 \end{bmatrix} = \begin{bmatrix} R_{ab} & P_{ab} \\ 0 & 1 \end{bmatrix} \begin{bmatrix} q_b \\ 1 \end{bmatrix} = \overline{g}_{ab}\overline{q}_{ab}, \quad \overline{g}_{ab} \in SE(3) \tag{2}$$

where $P_{ab} \in \mathbb{R}^3$ is the translation vector that starts from the origin of frame B relative to the origin of frame A; $R_{ab} \in \mathbb{R}^3 \times 3$ is an orthogonal matrix that represents the rotation of frame B relative to frame A.

The commonly used frame rotation expression is quaternion. Unlike the Euler angle, quaternion does not suffer from singularities. Besides, quaternion is computationally more efficient than the conventional rotational matrix representation. Quaternion generalizes a four-dimensional vector $q = q_0 + q_1 i + q_2 j + q_3 k = (q_0, \overrightarrow{q})$, where q_0 is the scalar part, and

q_1, q_2 and q_3 are the weighted values on the basis elements. In the coordinate rotation, vector q has the following representation:

$$q = \left(\cos\frac{\theta}{2}, \sin\frac{\theta}{2}\cos\omega_x, \sin\frac{\theta}{2}\cos\omega_y, \sin\frac{\theta}{2}\cos\omega_z \right) \tag{3}$$

where $(\cos\omega_x, \cos\omega_y, \cos\omega_z)$ represents the quaternion axis; θ symbolizes the angle around the quaternion axis.

For every homogeneous matrix $\overline{g}_{ab}$, there always exists a corresponding twist in the tangent space $se(3)$ where

$$se(3) = \{(v, \hat{\omega}) : v \in \mathbb{R}^3, \hat{\omega} \in so(3)\} \tag{4}$$

$$so(3) = \{S \in \mathbb{R}^{3\times 3} : S^T = -S\} \tag{5}$$

Let $\hat{\xi}$ be the twist, which is denoted as

$$\hat{\xi} = \begin{bmatrix} v \\ \hat{\omega} \end{bmatrix} = \begin{bmatrix} \hat{\omega} & v \\ 0 & 0 \end{bmatrix} \in se(3) \tag{6}$$

The variable $v = -\omega \times g$ represents the velocity of the point; g represents the distance between the root joint and the object joint. $\hat{\omega}$ is a skew-symmetric matrix which is defined as

$$\hat{\omega} = \begin{bmatrix} 0 & -\omega_3 & \omega_2 \\ \omega_3 & 0 & -\omega_1 \\ -\omega_2 & \omega_1 & 0 \end{bmatrix}, \quad \omega = [\omega_1, \omega_2, \omega_3]^T \tag{7}$$

The exponential product of $\hat{\xi}\theta$ is an element that belongs to $se(3)$ which is given by

$$e^{\hat{\xi}\theta} = \begin{cases} \begin{bmatrix} e^{\hat{\omega}\theta} & \left(I - e^{\hat{\omega}\theta}\right)\left(\hat{\omega}v + \omega\omega^T v\theta\right) \\ 0 & 1 \end{bmatrix}, & \omega \neq 0 \\ e^{\hat{\xi}\theta} = \begin{bmatrix} I & v\theta \\ 0 & 1 \end{bmatrix}, & \omega = 0 \end{cases} \tag{8}$$

If we define $g_{global,n}(0)$ as the initial configuration of a rigid body in reference n relative to the global frame, then the final configuration is given by:

$$g_{global,n}(\theta) = e^{\hat{\xi}\theta} g_{global,n}(0) \tag{9}$$

$e^{\hat{\xi}\theta}$ can be calculated via Equation (9) and the Rodrigues' formula:

$$e^{\hat{\omega}\theta} = I + \hat{\omega}\sin\theta + \hat{\omega}^2(1 - \cos\theta) \tag{10}$$

3. **Coordinate Transformation.** In order to verify the inertial motion tracking accuracy, we take advantage of the visual tracking device: *OptiTrack* to assist the arm motion capture as *OptiTrack* system tracking error is less than 1mm. The experiment is conducted by keeping inertial tracking records as well as those of *OptiTrack* tracking records frame by frame simultaneously.

The problem of interests is to transform the joint position in inertial coordinate frame to the corresponding position in *OptiTrack* coordinate frame. For this reason, the coordinate transformation is conducted. The scale factor K_0, the rotation matrix R and coordinate translation parameters (X_0, Y_0, Z_0) need to be determined.

Three points P_1, P_2, P_3 are denoted as the shoulder joint, elbow joint and wrist joint respectively. The IMU coordinate frame is defined as $O - XYZ$. *OptiTrack* coordinate frame is defined as $O' - X'Y'Z'$. $(x_i, y_i, z_i)_{i=1,2,3}$ represents coordinate of P_i in $O - XYZ$ frame. In a similar way, $(x_i', y_i', z_i')_{i=1,2,3}$ represents the coordinate of P_i in $O' - X'Y'Z'$ frame.
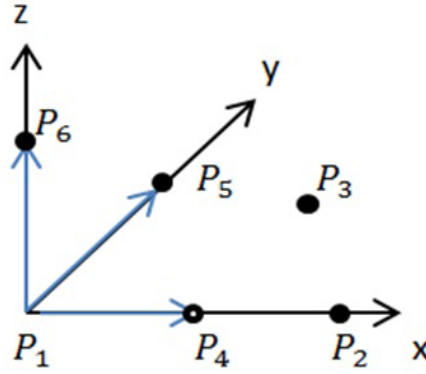
FIGURE 1. $P_1 - XYZ$ coordinate frame

3.1. **Scale factor k_0.** The difference of coordinate length basis gives rise to the parameter k_0. Here we define S_{ij} as the distance between P_i and P_i in $O - XYZ$ coordinate frame and S'_{ij} as the distance between P_i and P_i in $O' - X'Y'Z'$ coordinate frame. Based on the above definition, we could determine the scale factor k_0 as follows

$$k_0 = \frac{S_{12}' + S_{13}' + S_{23}'}{S_{12} + S_{13} + S_{23}} \tag{11}$$

3.2. **Transaction matrix derivation.** A new coordinate frame $P_1 - XYZ$ is defined in which P_1 is the origin and vector $\overrightarrow{P_1 P_2}$ lies on X-axis. After normalization, we obtain $\overrightarrow{P_1 P_4} = \frac{\overrightarrow{P_1 P_2}}{\|\overrightarrow{P_1 P_2}\|} = (a_1, b_1, c_1)$. As we can see from Figure 1, the product of $\overrightarrow{P_1 P_2} \times \overrightarrow{P_1 P_3}$ lies on Z-axis. After normalization, $\overrightarrow{P_1 P_6} = (a_2, b_2, c_2)$. Similarly, the cross product of $\overrightarrow{P_1 P_6} \times \overrightarrow{P_1 P_4}$ renders the normalized vector $\overrightarrow{P_1 P_5} = (a_3, b_3, c_3)$. Since $\overrightarrow{P_1 P_6}$ and $\overrightarrow{P_1 P_4}$ are normalized, the cross product is still normalized to both of these two vectors. Conspicuously, $\overrightarrow{P_1 P_5}$ lies on Y-axis in $P_1 - XYZ$ coordinate frame. In $P_1 - XYZ$ coordinate frame, $\overrightarrow{P_1 P_4}$, $\overrightarrow{P_1 P_5}$, $\overrightarrow{P_1 P_6}$ are the normal vectors along i, j, k axes.

By means of this strategy, we can also obtain the transformation matrix $R_{O'P_1}$ between $P_1 - X'Y'Z'$ and $O' - X'Y'Z'$.

Finally, the transformation matrix between frame $O - XYZ$ and frame $O' - X'Y'Z'$ is given by

$$R = R_{OP_1} \times R_{O'P_1}^{-1} \tag{12}$$

where R_{OP_1} symbolizes the matrix as follows:

$$R_{op1} = \begin{bmatrix} a_1 & a_2 & a_3 \\ b_1 & b_2 & b_3 \\ c_1 & c_2 & c_3 \end{bmatrix} \tag{13}$$

3.3. **Translation vector derivation.** Given the above derived scale factor k_0 and matrix R, we can easily deduce the translation parameters. The point P is arbitrarily chosen of which (x_p, y_p, z_p) and (x'_p, y'_p, z'_p) represent the coordinates in $O - XYZ$ and $O' - X'Y'Z'$ coordinate frames respectively. Then the translation vector $T = (x_0, y_0, z_0)^T$ is given by

$$\begin{pmatrix} x_0 \\ y_0 \\ z_0 \end{pmatrix} = \begin{pmatrix} x_p \\ y_p \\ z_p \end{pmatrix} - k_0 R \begin{pmatrix} x_p' \\ y_p' \\ z_p' \end{pmatrix} \tag{14}$$

4. **Experimental Results and Analysis.** To evaluate the performance of our proposed approach for image-pair outlier removal and orientation estimate, we conduct several experiments. In this section, our wearable inertial based motion tracking system and
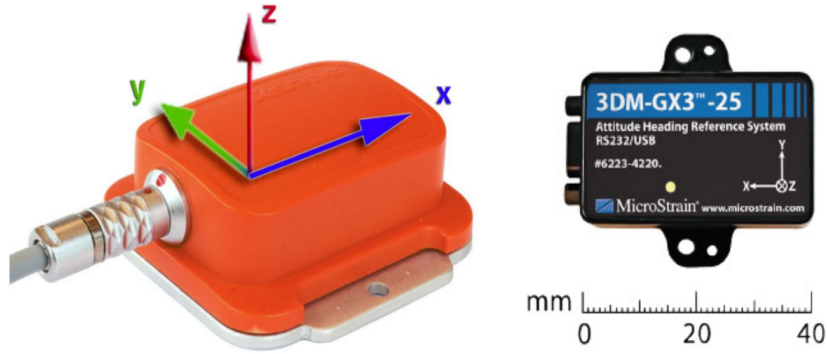
FIGURE 2. Xsens inertial sensor

FIGURE 3. Inertial measurement unit

OptiTrack visual tracking system are listed, and the experimental results and analysis are given as follows.

4.1. **System setup.** In our inertial based motion tracking system, three commercial Xsens MTi-G-700 inertial sensors are adopted as shown in Figure 2. Orientation and velocity increments are sampled at 400Hz.

Additionally, our research group also developed the IMU, which is 2.5cm in width and 5.6cm in length, shown in Figure 3. It samples the data at 60Hz and the inertial data that include accelerations, gyro rates and quaternions, are transmitted to the computer through wireless Bluetooth technology.

4.2. **Experiments and analysis.** In this section, the arm motion tracking process is introduced. The parameters we have to determine beforehand are the lengths of forearm and lower arm. Besides, the initial positions of inertial sensors mounted adjacent to the wrist, elbow and shoulder need also be measured. The unique data to be processed is quaternion. Here we use MATAB2012b to process the inertial data and use *OptiTrack* studio to process the visual data in recovering the arm motion process.

For verifying our wearable inertial tracking system accuracy, we take advantage of *OptiTrack* visual tracking records while conducting the inertial tracking simultaneously. The problem we encountered is the frame alignment between IMU coordinate and *OptiTrack* coordinate. Due to that reason, a local minimization solution is derived as follows:

$$\min_{i,j} \sum_{k=1}^{3} \omega_k \|P_k(i) - P_k(j)\|_2$$
$$\text{s.t.} \ \sum_{k=1}^{3} \omega_k = 1 \tag{15}$$

where $k = 1, 2, 3$ represents the shoulder, elbow, wrist joint respectively. ω_k represents the weighted value on the 2-norm distance between $P_k(i)$ and $P_k(j)$ of which i represents the frame number in inertial coordinate frame and j represents the frame number in *OptiTrack* coordinate frame. In this experiment, we set $\omega_1 = 0.6$, $\omega_2 = 0.3$, $\omega_3 = 0.1$. The weight values are set according to the joint movement space. The larger the joint movement space is, the lower value the weight will be, for the reason that the large movement will result in relatively obvious errors.
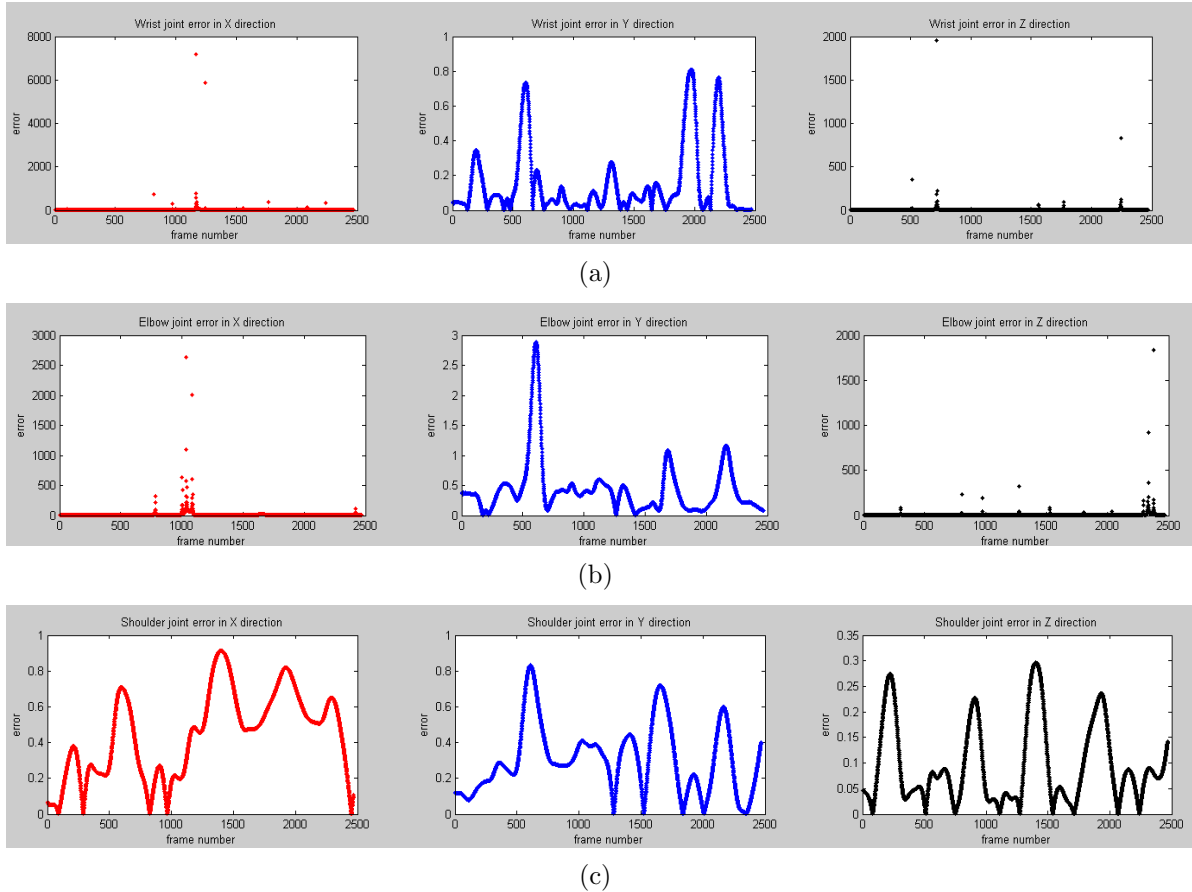

FIGURE 4. Arm joint position error: (a) tri-axial wrist joint error; (b) tri-axial elbow joint error; (c) tri-axial shoulder joint error

In our experiment, the visual tracking system *OptiTrack* data serve as the benchmark to validate our proposed inertial based motion tracking system accuracy. As can be seen, Figure 4 depicts the joint errors in X-, Y-, Z-axes respectively with respect to wrist joint, elbow joint and shoulder joint. From these three figures, we can see that wrist errors are pretty unpredictable in X and Z directions. Some of the deflection points are due to the sensor noise and the soft tissue artifacts.

5. **Conclusions.** In this paper, we have proposed an approach for inertial based arm motion tracking method. Lie algebra: twists and exponential maps are applied to recovering the arm motion process using the quaternions and pre-measured upper-arm and forearm length. *OptiTrack* visual tracking device fixed in the lab is utilized to track the arm motions. Based on the fact that the *OptiTrack* tracking accuracy is dramatically elegant, we evaluate the inertial motion tracking system in reference to vision tracking. Coordinate transformation that the positions of arm joints in inertial frame are transformed to the corresponding positions in the *OptiTrack* visual frame is done. Relative error analysis shown above validates the feasibility of our proposed inertial motion tracking system.

In the future, the arm motion tracking that lessens the body soft tissue artifacts will be studied and the corresponding experiments will be conducted.

REFERENCES

[1] H. Zhou, H. Hu and N. Harris, Application of wearable inertial sensors in stroke rehabilitation, *Proc. of the 27th Annual International Conference of the Engineering in Medicine and Biology Society*, Shanghai, China, pp.6825-6828, 2005.

[2] L. Tong, Q. Song, Y. Ge et al., HMM-based human fall detection and prediction method using tri-axial accelerometer, *Sensors Journal*, vol.13, no.5, pp.1849-1856, 2013.

[3] Z. Q. Zhang and J. K. Wu, A novel hierarchical information fusion method for three-dimensional upper limb motion estimation, *IEEE Trans. Instrumentation and Measurement*, vol.60, no.11, pp.3709-3719, 2011.

[4] A. Perttula, H. Leppakoski, M. Kirkko-Jaakkola et al., Distributed indoor positioning system with inertial measurements and map matching, *IEEE Trans. Instrumentation and Measurement*, vol.63, no.11, pp.2682-2695, 2014.

[5] Y. Zhang, W. Liang, J. Tan et al., PCA and HMM based arm gesture recognition using inertial measurement unit, *Proc. of the 8th International Conference on Body Area Networks*, pp.193-196, 2013.

[6] S. Sabatelli, M. Galgani, L. Fanucci et al., A double-stage Kalman filter for orientation tracking with an integrated processor in 9-D IMU, *IEEE Trans. Instrumentation and Measurement*, vol.62, no.3, pp.590-598, 2013.

[7] R. G. J. Damgrave and D. Lutters, The drift of the xsens moven motion capturing suit during common movements in a working environment, *Proc. of the 19th CIRP Design Conference – Competitive Design*, 2009.

[8] S. O. H. Madgwick, A. J. L. Harrison and R. Vaidyanathan, Estimation of IMU and MARG orientation using a gradient descent algorithm, *IEEE International Conference on Rehabilitation Robotics*, pp.1-7, 2011.

[9] X. Chen, J. Zhang, W. R. Hamel et al., An inertial-based human motion tracking system with twists and exponential maps, *Proc. of IEEE International Conference on Robotics and Automation (ICRA)*, Hong Kong, China, pp.5665-5670, 2014.

[10] A. G. Cutti, A. Giovanardi, L. Rocchi, A. Davalli and R. Sacchetti, Ambulatory measurement of shoulder and elbow kinematics through inertial and magnetic sensors, *Medical and Biological Engineering and Computing*, vol.46, no.2, pp.169-178, 2008.

[11] *http://www.optitrack.com/*.

[12] M. El-Gohary, S. Pearson and J. McNames, Joint angle tracking with inertial sensors, *The 30th Annual International Conference of the IEEE*, pp.1068-1071, 2008.

[13] R. Zhu and Z. Zhou, A real-time articulated human motion tracking using tri-axis inertial/magnetic sensors package, *IEEE Trans. Neural Systems and Rehabilitation Engineering*, vol.12, no.2, pp.295-302, 2004.

[14] R. M. Murray, Z. Li, S. S. Sastry and S. S. Sastry, *A Mathematical Introduction to Robotic Manipulation*, CRC Press, 1994.